Electronic Supplementary Material (ESI) for Physical Chemistry Chemical Physics.

Experimental and Theoretical Methods

The reactions of CH_2OO, CH_3CHOO, $(CH_3)_2COO$ and CH_3CH_2CHOO Criegee intermediates with carboxylic acids are investigated in the present study. Deuterated formic or acetic acid [DCOOD (Sigma Aldrich, 95 wt. % in D_2O, 98 atom %D), CD_3COOD (Sigma Aldrich, 99% purity, 99.5 atom %D) or CH_3COOD (Sigma Aldrich, 99% purity, 99 atom %D)] is injected upstream of the pulsed valve and its vapor is entrained in 20% O_2/Ar carrier gas (25 psi). In some experiments, normal formic acid (Acros, 99% purity) or acetic acid (Fisher, glacial, 99.9% purity) is utilized. The vapor from one of the diiodoalkane precursors (CH_2I_2, CH_3CHI_2, $(CH_3)_2CI_2$ and $CH_3CH_2CHI_2$) is introduced into the gas stream immediately before the pulsed valve. Other than CH_2I_2 (Alfa Asear, 99% purity), the precursors CH_3CHI_2, $(CH_3)_2CI_2$ and $CH_3CH_2CHI_2$ are synthesized as in prior work.[1] The gas mixture is pulsed through a solenoid valve into a quartz capillary tube (1 mm ID, 3 mm OD) reactor.

The generation of the Criegee intermediates is analogous to earlier studies in this laboratory.[1-3] Radiation from a KrF excimer laser at 248 nm (Coherent, Complex 102, 80 mJ, 5 Hz) is loosely focused with a cylindrical lens on the capillary tube, irradiating about half of its length (36 mm) closest to the pulsed valve. The precursor is photolyzed by the excimer laser, yielding an alkyl iodide radical product that subsequently reacts with O_2 to form the Criegee intermediates. The Criegee intermediates may also undergo further reaction with carboxylic acid in the gas mixture as it flows through the capillary tube into the vacuum chamber.

The Criegee intermediates and other products, including vinyl hydroperoxide, are collisionally stabilized and thermalized in the capillary tube, cooled in a supersonic expansion, and travel ~4 cm downstream into the ionization region of a time-of-flight mass spectrometer (TOF-MS). Both Criegee intermediates and vinyl hydroperoxide products are detected by photoionization using focused fixed-frequency VUV radiation at 118 nm under collision-free conditions. The VUV is generated by frequency tripling the third harmonic output of a Nd:YAG laser (Continuum Powerlite 9000, 355 nm, 20 mJ, 10 Hz)

in a phase-matched Xe/Ar gas mixture. The TOF-MS is processed with a digital oscilloscope (LeCroy WaveRunnner 6050A) and transferred to a laboratory computer for further analysis.

Photoionization signals that are not dependent on excimer photolysis are subtracted from the mass spectra using an active background subtraction scheme; the excimer photolysis pulse (5 Hz) is present for every other VUV photoionization laser pulse (10 Hz). The TOF mass spectra are recorded for mass channels (m/z) ranging from 0 to 200 amu. Although 248 nm photolysis causes some fragmentation of the precursor and/or carboxylic acid that can be seen in lower mass channels, the present study focuses on the Criegee intermediates and adjacent mass channels. Yet higher masses that might correspond to a potential adduct between the Criegee intermediate and carboxylic acid are not detected in the TOF spectrum. Neither formic nor acetic acid are photoionized at 10.5 eV.[4, 5]

Although CH_3CHOO and CH_2=CHOOH/D are expected to be ionized by single photon VUV excitation at 118 nm (10.5 eV), many other of their isomers may not be photoionized. The latter include methyl dioxirane (VIE=10.8 eV; AIE=10.36 eV),[6] glycolaldehyde $HOCH_2$-CH=O (10.86 eV, dissociative ionization),[7] acetic acid (AIE=10.70 eV), and methyl formate (AIE=10.85 eV), which have ionization energies above 10.5 eV and will not be detected using 118 nm VUV radiation for ionization. One additional isomer is bis(oxy) $CH_3CH(O)_2$, for which the AIE is predicted at 10.38 eV;[6] however, this isomer has not been observed in previous studies[6, 8] and seems to be an implausible product in the current study. For $(CH_3)_2COO$ and CH_3CH_2CHOO, other stable isomers exist with ionization potentials less than 10.5 eV, such as methyl acetate (10.25 eV) and propionic acid (10.44 eV); these products are not expected to be formed directly in the carboxylic acid reactions.

For UV-induced depletion studies, an unfocused UV laser at 300 nm (~2 mJ) is introduced ~100 ns prior to the VUV photoionization laser in a counter-propagating and spatially overlapped configuration. The UV radiation is generated by frequency-doubling the output of a Nd:YAG (Continuum

Powerlite 7020, 532 nm) pumped dye laser (Continuum ND6000) utilizing Rhodamine 640 dye and calibrated with

a wavemeter (Coherent Wavemaster).

For organic hydroperoxides, previous experimental studies indicate absorption cross sections on the order of 10^{-21} cm^2 $molec^{-1}$ at 300 nm, which is 5 orders of magnitude lower than that of the Criegee intermediates (10^{-17} $cm^2 molec^{-1}$).[9] Their absorption cross sections increase substantially (ca. 2 orders of magnitude) at 200 nm.[10] Although the computed vertical excitation energies for various vinyl hydroperoxides lie near 200 nm (see Table S2), one may still anticipate very weak absorption for vinyl hydroperoxides at 300 nm (by analogy to other organic hydroperoxides), which is not detected in depletion measurements.

All electronic structure calculations reported here have been performed using the NWChem[11] and Gaussian09[12] programs. We have examined the reactions of *syn*-CH_3CHOO, *syn*-CH_3CH_2CHOO and $(CH_3)_2COO$ with carboxylic acids, HCOOH, CH_3COOH, and CH_3CH_2COOH. For the reaction of *syn*-CH_3CHOO with the simplest carboxylic acid, HCOOH, all the possible pathways were investigated. However, for the reactions of *syn*-CH_3CHOO with larger carboxylic acids, only low-energy or nearly barrierless pathways were calculated. For larger Criegee Intermediates, *syn*-CH_3CH_2CHOO and $(CH_3)_2COO$, only low-energy pathways were calculated. The structures of all species were fully optimized at the M06-2X/aug-cc-pVTZ level of theory and the nature of each stationary point (minimum or saddle point) was verified by a vibrational frequency analysis. For the reaction of *syn*-CH_3CHOO with the simplest carboxylic acid, HCOOH, the energy of the minima and transition states for the lower barrier pathways were recalculated at the CCSD(T)/aug-cc-pVTZ//M06-2X/aug-cc-pVTZ level; the resulting relative energies were within 0.5-2.5 kcal/mol of the M06-2X energies in all cases.[13] Vertical ionization energies (VIEs) (Table S1) were calculated using the cation energy at the optimized geometry of the corresponding neutral molecule, while the adiabatic ionization energies (AIEs) (Table S1) were calculated from the

energy difference between the optimized geometries of the cation and neutral. The calculated AIEs are corrected for zero-point vibrational effects. Finally, the UV-vis absorption wavelengths for various VHPs (Table S2) were calculated at the TD-B3LYP/6-311+G(2d,p)//B3LYP/6-311+G(2d,p), TD-M06-2X/aug-cc-pVTZ//M06-2X/aug-cc-pVTZ, and EOMCCSD/aug-cc-pVTZ//M06-2X/aug-cc-pVTZ levels of theory.

Recently reported photoionization efficiency curves for HPMF on the very weak parent mass and stronger fragment channels indicate an ionization threshold for HPMF of 10.05 $\pm$ 0.05 eV.[14] An AIE near 10.05 eV has been predicted for several conformers of HPMF, although a much higher (~1.2 eV) VIE is expected due to the large geometry change between the ground and cationic state.[14] A similarly large change between the VIE and AIE is predicted here for HPEF (Table S1), suggesting that only a weak photoionization signal will be observed near the AIE.

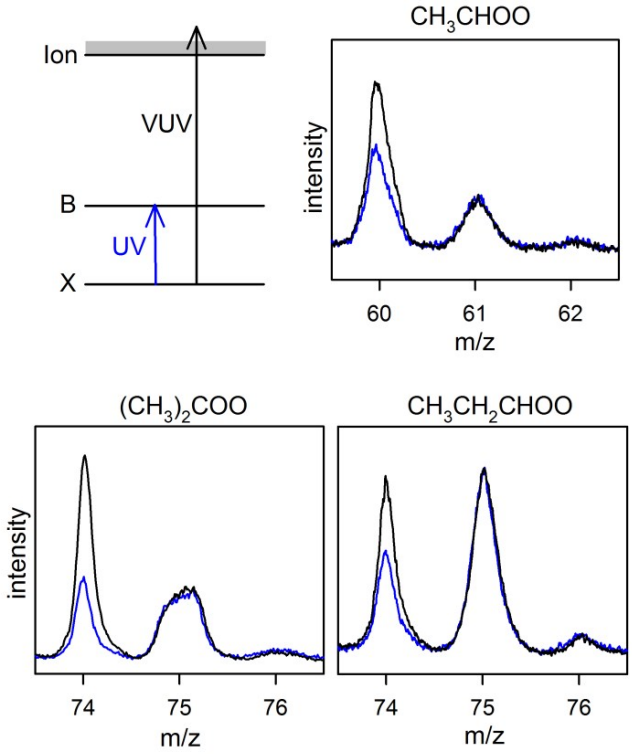

Figure S1. VUV photoionization and resultant time-of-flight mass spectra upon reaction of CD_3COOD with CH_3CHOO (m/z 60), $(CH_3)_2COO$ (m/z 74), CH_3CH_2CHOO (m/z 74) Criegee intermediates (black), and their partially deuterated vinyl hydroperoxide (VDP) products CH_2=CHOOD, CH_2=C(CH_3)OOD, and CH_3CH=CHOOD (black). Upon UV irradiation at 300 nm (blue), the Criegee intermediate signal is significantly depleted (~50%) due to UV excitation on the strong B-X transition that removes population from the ground state prior to VUV photoionization, while the VDP signal is unchanged. The slight broadening of VDP mass peaks (m/z 61 and 75) is attributed to a small velocity component (ca. 30 m/s based on SIMION simulations[15]) of the newly formed VDP products orthogonal to the molecular beam axis.

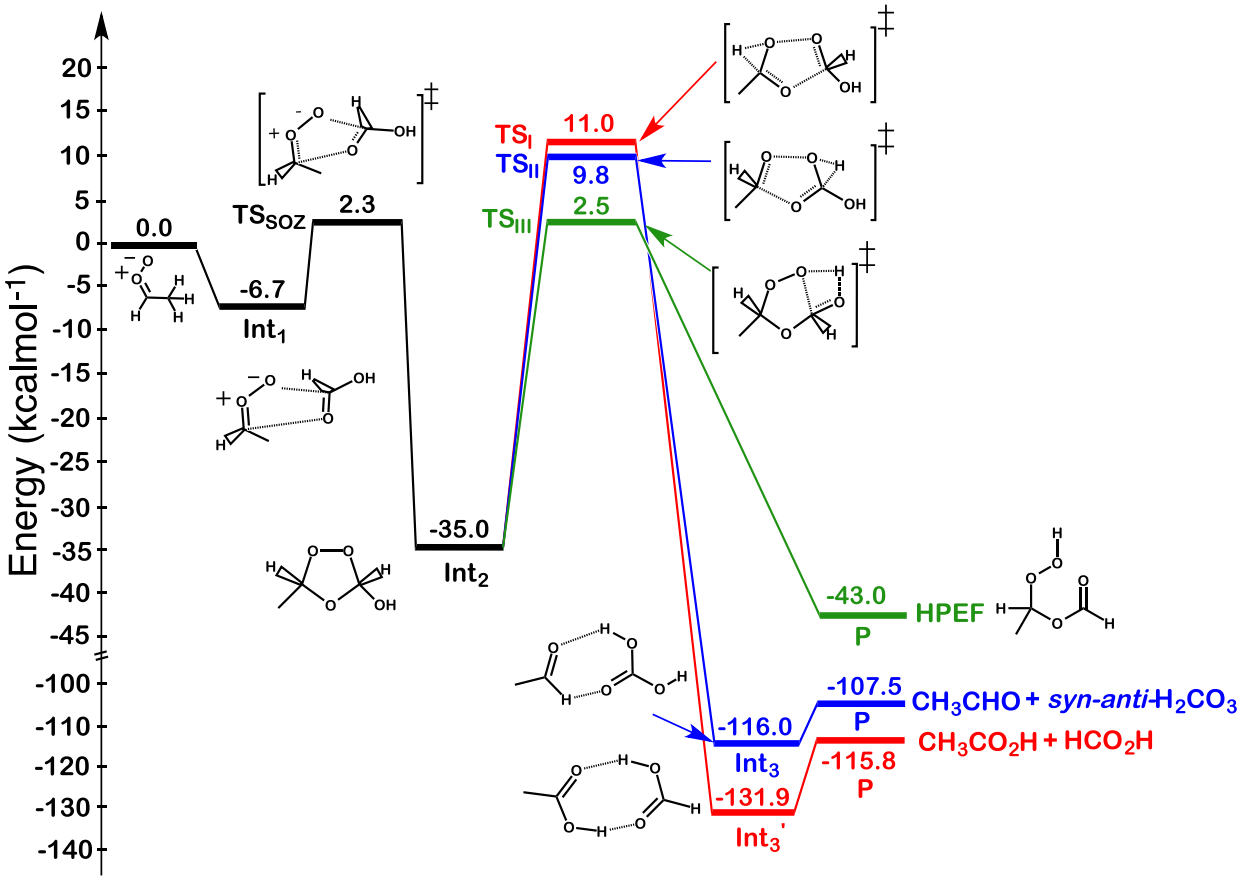

Figure S2. M06-2X/aug-cc-pVTZ calculated electronic energy profile for the reaction of *syn*-CH_3CHOO with HCOOH involving the formation of *cis*-secondary ozonide-type species.

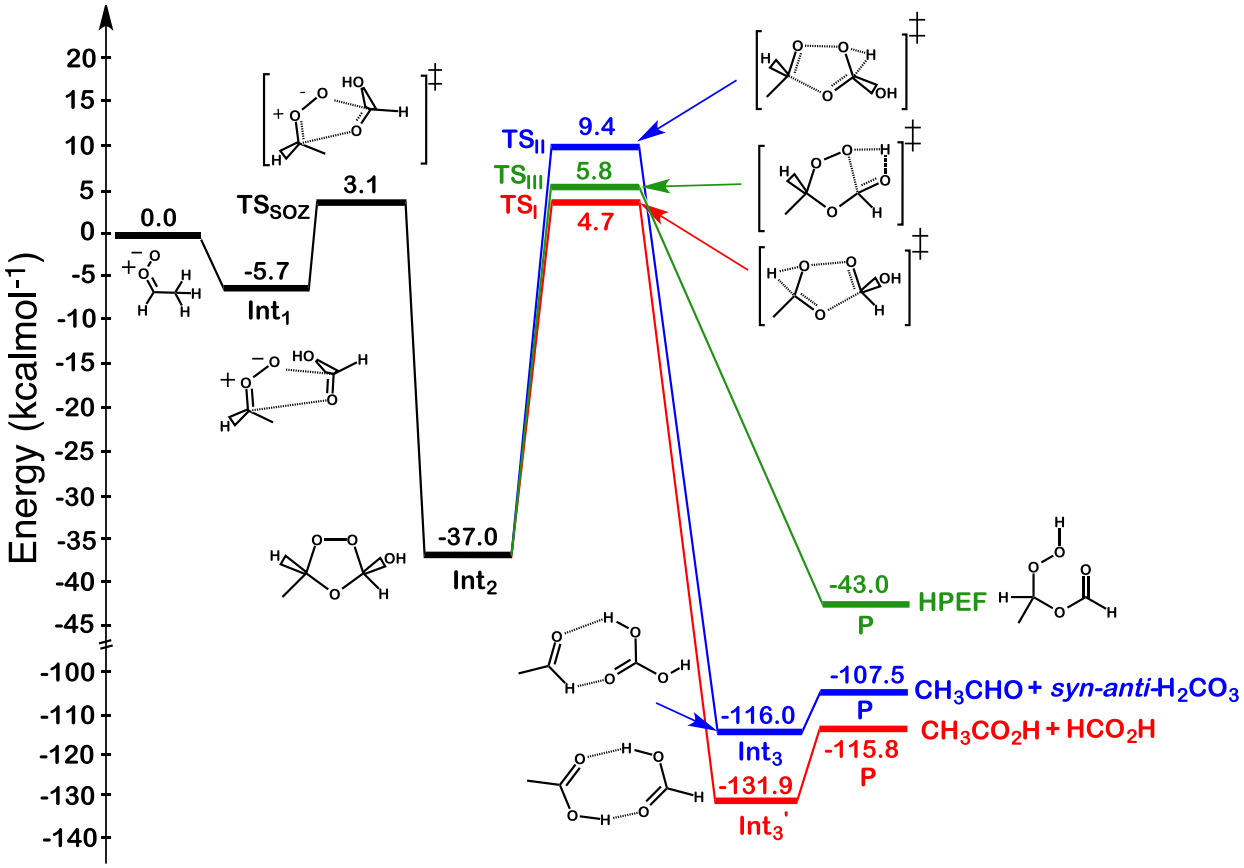

Figure S3. M06-2X/aug-cc-pVTZ calculated electronic energy profile for the reaction of *syn*-CH_3CHOO with HCOOH involving the formation of *trans*-secondary ozonide-type species.

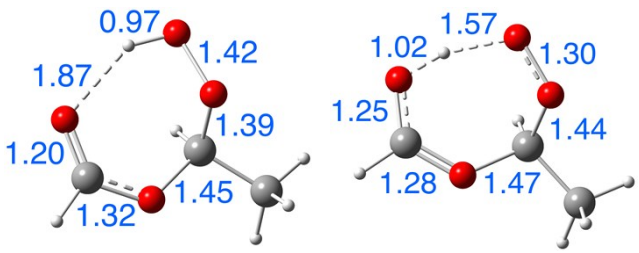

Figure S4. M06-2X/aug-cc-pVTZ calculated geometries of neutral (*left*) and cationic (*right*) hydroperoxy ethyl formate. Key bond distances (in Å) are also shown.

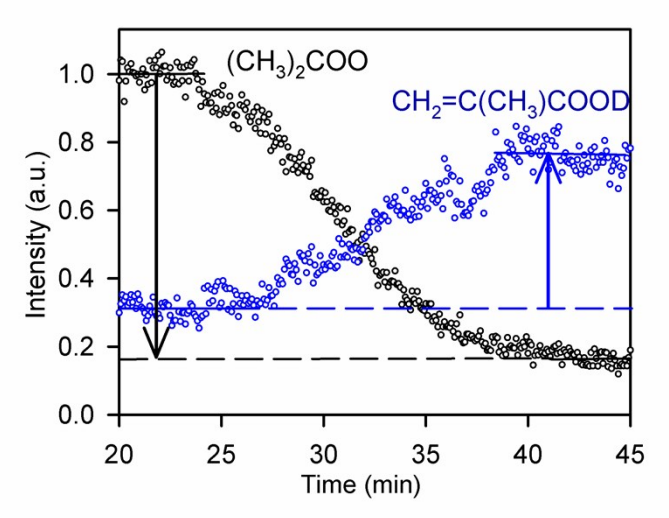

Figure S5. Photoionization TOF-MS signal intensities for the $(CH_3)_2COO$ Criegee intermediate (m/z 74, black) and the $CH_2=C(CH_3)COOD$ VDP product (m/z 75, blue) as a function of time after injecting deuterated acetic acid CD_3COOD into the carrier gas upstream of the pulsed valve. A trace amount of CD_3COOD was introduced to the system for initial optimization of experimental conditions, resulting in a nonzero baseline of VDP at early time. A concomitant decrease in the Criegee intermediate (black arrow) and increase in the VDP product (blue arrow) signal is observed, indicating that as much as 50% of Criegee intermediates are converted to VDP, assuming equal ionization cross sections for the Criegee intermediate and VDP at 10.5 eV.

Table S1. Vertical and adiabatic ionization energies of key species. The present calculations were carried out at the CCSD(T)/aug-cc-pVTZ//M06-2X/aug-cc-pVTZ level of theory. The numbers in blue are calculated at the M06-2X/aug-cc-pVTZ level of theory.

Species		*Cal.*				*Exp.*
		Present		*Previous*		
		Vertical	*Adiabatic*	*Vertical*	*Adiabatic*	
Criegee Intermediate	*syn*-CH_3CHOO	9.42 (9.33)	9.28	9.49[6]	9.38[6]	9.4[8]
	syn-CH_3CH_2CHOO	9.17		9.14[1]		
	$(CH_3)_2COO$	8.79		8.71[1]		
Vinyl Hydroperoxide	CH_2=CHOOH	9.60 (9.61)	9.09	9.51[6]	9.18[6]	
	$CH(CH_3)$=CHOOH	9.05				
	CH_2=$C(CH_3)$OOH	9.25				
Carboxylic Acid	HCOOH	11.52 (11.63)	11.23			11.3[4]
	CH_3COOH	10.88 (10.96)	10.55			10.7[5]
	CH_3CH_2COOH	10.82				
Hydroperoxy Alkyl Ester	$CH_3CH(OOH)OC(O)H$ (HPEF)	10.87 (10.98)	9.39			
	$CH_3CH(OOH)OC(O)CH_3$ (HPEA)	10.69				
	$CH_3CH(OOH)OC(O)CH_2CH_3$ (HPEP)	10.62				
	$CH_3CH_2CH(OOH)OC(O)H$ (HPPF)	10.91				
	$CH_3CH_2CH(OOH)OC(O)CH_3$ (HPPA)	10.65				
	$CH_3CH_2CH(OOH)OC(O)CH_2CH_3$ (HPPP)	10.57				
	$(CH_3)(CH_3)C(OOH)OC(O)H$ (HPiPF)	10.84				
	$(CH_3)(CH_3)C(OOH)OC(O)CH_3$ (HPiPA)	10.59				
	$(CH_3)(CH_3)C(OOH)OC(O)CH_2CH_3$ (HPiPP)	10.52				

Table S2. Calculated vertical-excitation UV absorption wavelengths for various vinyl hydroperoxides (VHPs) studied in the present work. The *EOM-CCSD/aug-cc-pVTZ* results are calculated from the M06-2X/aug-cc-pVTZ optimized geometries.

VHP	**UV Absorption (nm)**		
	TD-B3LYP/6-311+G(2d,p)	*TD-M06-2X/aug-cc-pVTZ*	*EOM-CCSD/aug-cc-pVTZ*
CH_2=CHOOH	195.5	215.8	204.2
CH_2=C(CH_3)OOH	214.2	216.5	205.6
(CH_3)CH=CHOOH	194.7	227.3	214.3

Table S3. M06-2X/aug-cc-pVTZ calculated energies of various species involved in the carboxylic acid-catalyzed gas-phase tautomerization of *syn*-CH_3CHOO, *syn*-CH_3CH_2CHOO, and $(CH_3)_2COO$ (298.15 K, 1 atm, kcal/mol). All energies are reported with respect to the separated reactants.

Criegee Intermediate	**Carboxylic Acid**	**Int_1**		**TS**		**Int_2**		**P**	
		ΔE	*ΔG*	*ΔE*	*ΔG*	*ΔE*	*ΔG*	*ΔE*	*ΔG*
syn-CH_3CHOO	Formic acid	-17.5	-7.1	-11.2	0.2	-31.8	-21.5	-21.9	-22.2
	Acetic Acid	-17.0	-6.9	-10.4	1.2	-32.3	-22.2	-21.9	-22.2
	Propionic acid	-18.1	-7.3	-11.3	0.6	-32.3	-21.9	-21.9	-22.2
syn-CH_3CH_2CHOO	Formic acid	-19.0	-8.6	-11.5	0.0	-33.7	-23.6	-23.7	-24.0
	Acetic Acid	-18.0	-6.9	-10.7	0.8	-34.0	-23.8	-23.7	-24.0
	Propionic acid	-19.0	-7.6	-11.6	0.3	-33.9	-23.4	-23.7	-24.0
$(CH_3)_2COO$	Formic acid	-20.4	-9.4	-12.5	-1.8	-29.2	-18.8	-18.7	-19.0
	Acetic Acid	-19.6	-8.9	-11.2	0.3	-29.9	-19.1	-18.7	-19.0
	Propionic acid	-20.5	-9.2	-11.9	0.1	-29.5	-18.6	-18.7	-19.0

Table S4. M06-2X/aug-cc-pVTZ calculated energies of various species involved in the hydroperoxy alkyl ester-forming gas-phase reaction of *syn*-CH_3CHOO, *syn*-CH_3CH_2CHOO, and $(CH_3)_2COO$ with carboxylic acids (298.15 K, 1 atm, kcal/mol). All energies are reported with respect to the separated reactants.

Criegee Intermediate	**Carboxylic Acid**	**Hydroperoxy Alkyl Ester (HPEA)**	**Reaction Energy**	
			ΔE	*ΔG*
syn-CH_3CHOO	Formic acid	$CH_3CH(OOH)OC(O)H$ (HPEF)	-43.0	-31.0
	Acetic Acid	$CH_3CH(OOH)OC(O)CH_3$ (HPEA)	-43.4	-31.3
	Propionic acid	$CH_3CH(OOH)OC(O)CH_2CH_3$ (HPEP)	-43.4	-31.3
syn-CH_3CH_2CHOO	Formic acid	$CH_3CH_2CH(OOH)OC(O)H$ (HPPF)	-41.5	-29.4
	Acetic Acid	$CH_3CH_2CH(OOH)OC(O)CH_3$ (HPPA)	-41.6	-29.2
	Propionic acid	$CH_3CH_2CH(OOH)OC(O)CH_2CH_3$ (HPPP)	-42.0	-29.2
$(CH_3)_2COO$	Formic acid	$(CH_3)(CH_3)C(OOH)OC(O)H$ (HPiPF)	-38.2	-25.5
	Acetic Acid	$(CH_3)(CH_3)C(OOH)OC(O)CH_3$ (HPiPA)	-38.1	-25.1
	Propionic acid	$(CH_3)(CH_3)C(OOH)OC(O)CH_2CH_3$ (HPiPP)	-38.4	-25.3

References

1. F. Liu, J. M. Beames, A. M. Green and M. I. Lester, *J. Phys. Chem. A*, 2014, **118**, 2298-2306.
2. J. M. Beames, F. Liu, L. Lu and M. I. Lester, *J. Am. Chem. Soc.*, 2012, **134**, 20045-20048.
3. J. M. Beames, F. Liu, L. Lu and M. I. Lester, *J. Chem. Phys.*, 2013, **138**, 244307.
4. C. R. Brundle, D. W. Turner, M. B. Robin and H. Basch, *Chem. Phys. Lett.*, 1969, **3**, 292-296.
5. D. A. Sweigart and D. W. Turner, *J. Am. Chem. Soc.*, 1972, **94**, 5592-5598.
6. C. A. Taatjes, O. Welz, A. J. Eskola, J. D. Savee, A. M. Scheer, D. E. Shallcross, B. Rotavera, E. P. F. Lee, J. M. Dyke, D. K. W. Mok, D. L. Osborn and C. J. Percival, *Science*, 2013, **340**, 177-180.
7. J. L. Holmes and F. P. Lossing, *Int. J. Mass Spectrom. Ion Processes*, 1984, **58**, 113-120.
8. O. Welz, J. D. Savee, D. L. Osborn, S. S. Vasu, C. J. Percival, D. E. Shallcross and C. A. Taatjes, *Science*, 2012, **335**, 204-207.
9. S. Hsieh, R. Vushe, Y. T. Tun and J. L. Vallejo, *Chem. Phys. Lett.*, 2014, **591**, 99-102.
10. M. Baasandorj, D. K. Papanastasiou, R. K. Talukdar, A. S. Hasson and J. B. Burkholder, *Phys. Chem. Chem. Phys.*, 2010, **12**, 12101-12111.
11. M. Valiev, E. J. Bylaska, N. Govind, K. Kowalski, K. P. Straatsma, H. J. J. van Dam, D. Wang, J. Nieplocha, E. Apra, T. L. Windus, W. A. de Jong, *NWChem: Comput. Phys. Commun.,* 2010, **181**, 1477-1489.
12. Gaussian, *Frisch, M. J. et al. Gaussian 09, revision C.02; Gaussian, Inc.: Wallingford, CT, 2009.*
13. M. Kumar, D. H. Busch, B. Subramaniam and W. H. Thompson, *Phys. Chem. Chem. Phys.*, 2014, **16**, 22968-22973.
14. K. Moshammer, A. W. Jasper, D. M. Popolan-Vaida, A. Lucassen, P. Diévart, H. Selim, A. J. Eskola, C. A. Taatjes, S. R. Leone, S. M. Sarathy, Y. Ju, P. Dagaut, K. Kohse-Höinghaus and N. Hansen, *J. Phys. Chem. A*, 2015, DOI: 10.1021/acs.jpca.5b00101.
15. D. A. Dahl, *Int. J. Mass spectrom.*, 2000, **200**, 3-25.